Fabrication of Quantum Dot-Polymer Composites: Semiconductor Nanoclusters in Dual-Function Polymer Matrices with Electron-Transporting and Cluster-Passivating Properties

D. E. Fogg,[†] L. H. Radzilowski,[‡] B. O. Dabbousi,[†] R. R. Schrock,*[,†] E. L. Thomas,[‡] and M. G. Bawendi[†]

Departments of Chemistry and Materials Science and Engineering, Massachusetts Institute of Technology, Cambridge, Massachusetts 02139

Received May 6, 1997; Revised Manuscript Received September 23, 1997[⊗]

ABSTRACT: Hybrid inorganic−organic polymer composites have been prepared by a convergent approach in which nearly monodisperse CdSe or (CdSe)ZnS nanoclusters are sequestered within phosphine-containing domains in a charge-transporting matrix. The motivation for these studies is the potential utility of such composites as combined electron-transport and emitter layers in light-emitting devices. Diblock copolymers with electronically passivating and charge-transport capabilities were prepared via ring-opening metathesis polymerization of octylphosphine- and oxadiazole-functionalized norbornenes. Independently prepared CdSe and ZnS-overcoated CdSe nanoclusters, surface-passivated by trioctylphosphine and trioctylphosphine oxide groups, are tethered by polymer-bound phosphine donors, resulting in immediate, sustained increases in fluorescence. Thin films of the CdSe-block copolymer composites, static-cast from dilute solution, exhibit microphase separation, with segregation of nanoclusters within phosphine-rich microdomains. Under similar conditions, (CdSe)ZnS clusters undergo macrophase separation. Rapid-casting techniques arrest morphological development at an earlier stage, giving small micelles of a few nanoclusters each in phosphine-containing domains. Dispersion of electronically passivated nanoclusters throughout a functionalized polymer matrix leads to composites with a broad range of potential applications, including light-emitting devices and photovoltaic cells.

Intense interest in new materials with electroluminescence properties that can be tuned at the molecular level is evident from the recent literature.[1−7] Semiconductor quantum dots (nanoclusters with diameters smaller than that of the bulk exciton)[8] exhibit electronic and optical properties dramatically different from the bulk material, most notably discrete absorption features that shift to higher energy with decreasing nanocluster size, and a "band edge" luminescence maximum that can then be tuned throughout the visible spectrum by variation of cluster size. Quantum dot-polymer composites hold great promise as hybrid organic/inorganic electroluminescent devices in which the emission wavelength is precisely specified by choice of nanocluster diameter.

Our previous efforts focused on development of composites containing near-monodisperse CdSe quantum dots in an electronically passivating, *insulating* polymer matrix.[9] A convergent approach, involving independent synthesis of nanoclusters and polymer, permitted us to exploit recently developed methods for the preparation of CdSe quantum dots with remarkably narrow size distributions.[10] These nanoclusters consist of a CdSe core, surface-capped with bulky $P(oct)_3$ and $O{=}P(oct)_3$ (oct = octyl) groups that enforce steric segregation of the clusters, preventing agglomeration. The capping groups also effect electronic passivation of the nanoclusters, and consequently promote high photoluminescence, by saturating the CdSe surfaces and preventing localization of photogenerated electron-hole pairs in coordinatively unsaturated surface sites. Good overlap is thus constrained between the carriers within the CdSe core, resulting in high rates of radiative recombination; quantum yields of ca. 10% are observed in room-temperature fluorescence experiments. The polymer hosts designed for these prefabricated clusters were diblock copolymers composed of a minority block of phosphine-functionalized repeat units coupled to a majority block of insulating hydrocarbon repeat units. Displacement of nanocluster capping groups by polymer-bound phosphine donors effectively tethered the clusters to the polymer backbone, sequestering them within phosphine-rich domains in the insulating block matrix. Immediate and sustained increases in fluorescence were observed for the clusters following incorporation, owing to electronic passivation by the polymer host.

We have since turned our attention to the problem of devising a modified, dual-function copolymer host in which passivating properties are supplemented by charge transport capabilities. Quantum dots in such a matrix can be used as fluorophores into which charge can be funnelled, giving access to electroluminescence applications and light-emitting devices (LEDs). These novel composites integrate the key advantages of molecularly-doped and all-polymer LEDs. Doping of inert polymers with molecular electroluminescent materials permits precise control over emitter:diluter ratios and facile tuning of emission wavelength.[2,6,11] Our approach combines these features with the excellent processability, film uniformity, and reduced tendency toward crystallization that constitute the principal advantages of all-polymer LEDs. Thus, the nanoclusters are treated as molecular dopants that are converted into an integral part of the polymer matrix by anchoring to the polymer backbone: the polymer-bound phosphine groups not only maintain the structural integrity and luminescent properties of the nanoclusters but also effect dispersion of clusters throughout the polymer matrix, limiting aggregation and attendant problems of crystallization. The exceptional functional diversity and precision of ring-opening metathesis polymerization (ROMP) techniques, which permit facile modification of polymer

[†] Department of Chemistry.
[‡] Department of Materials Science and Engineering.
[⊗] Abstract published in *Advance ACS Abstracts,* December 15, 1997.

S0024-9297(97)00626-8 CCC: $14.00

Table 1. Physical Data for Polymers

polymer[a]	yield	MW (theory)	M_n (found; high-MW peak)	PDI[b]	M_n (found; low-MW peak)	PDI[c]
$[NBPBD]_{300}$	89	151 600			157 600	1.02
$[NBPBD]_{300}[NBP]_{20}$	90	160 600	324 500	1.02	165 500	1.03
$[NBPBD]_{300}[NBP]_{20}$[d]	89	160 600			171 200	1.07

[a] All polymers were prepared in THF, using $Mo(CHMe_2Ph)(NAr)(O\text{-}t\text{-}Bu)_2$ as initiator. Theoretical MW values are based on 100% conversion of monomer and complete consumption of initiator, allowing for $PhMe_2CCH=$ and $=CHPh$ end groups. M_n (found) was determined by light-scattering (from M_w/PDI). [b] Polydispersity index, M_w/M_n, for higher molecular weight peak. [c] Polydispersity index, M_w/M_n, for lower molecular weight pack. [d] Polymer prepared after degassing monomer **1** by stirring under dynamic vacuum for 8 h.

structure via synthesis of suitably functionalized norbornene monomers, give ready access to polymers that combine these features with the requisite electron-transport capabilities, containing an alkylphosphine moiety within one block[12] and an oxadiazole moiety within the other.[9] Oxadiazole derivatives, almost invariably in molecular form, have been widely used as electron-transport materials in devices incorporating both quantum dots[5] and traditional organic chromophores.[7,13,14] Polymeric versions of these useful materials have recently been reported by us[12] and others.[15,16]

In this paper we report the synthesis of diblock ROMP polymers containing oxadiazole- and octylphosphine-functionalized polynorbornene blocks, and fabrication of polymer−nanocluster composites via incorporation of CdSe quantum dots. Composites containing modified quantum dots[17] in which the CdSe core is overcoated with a thin shell of ZnS are also described. The latter, hybrid clusters exhibit photoluminescence quantum yields an order of magnitude higher than those found for the original CdSe nanoclusters, owing to further confinement of the exciton by the higher-bandgap ZnS shell.[17−19] Solution fluorescence is enhanced for both cluster types following incorporation into phosphine-functionalized polymers. Enhanced fluorescence indicates an increase in electronic passivation and, by inference, good affinity of the phosphine donors for both CdSe and ZnS surface sites. Transmission electron microscopic (TEM) characterization of slow-cast thin films of the composites reveals segregation of CdSe clusters within a network of phosphine-rich domains. In contrast, the ZnS-overcoated clusters evince a strong self-affinity, manifest in a tendency toward macrophase separation, under conditions that permit approach to equilibrium morphologies. Rapid-casting techniques intercept morphological development at an earlier stage, which presumably resembles more closely the level of assembly present in solution. TEM characterization of the latter films suggest little phase separation but formation of micelle like structures with aggregates of a few clusters within small phosphine domains.

Preliminary electroluminescence studies suggest considerable promise for these materials as combined electron-transport and emitter layers in light-emitting devices incorporating self-assembled hole-transport platforms. Detailed studies of heterostructured devices, optimized for composition and morphology, will be reported separately.[20]

Experimental Section

General. All experiments, unless otherwise noted, were performed under a nitrogen atmosphere in a Vacuum Atmosphere drybox or by using standard Schlenk/vacuum line techniques. Hexane, toluene, and tetrahydrofuran (THF) for polymerization were distilled from purple sodium benzophenone ketyl under nitrogen and then stored in the drybox over activated 4 Å molecular sieves. Methanol was degassed by sparging with argon for 30 min prior to use. Benzaldehyde was distilled under argon, degassed by three freeze−pump−thaw cycles, and then stored at −40 °C in the drybox. The ROMP initiator $Mo(CHCMe_2Ph)(NAr)(O\text{-}t\text{-}Bu)_2$ (where Ar = $2,6\text{-}C_6H_3\text{-}i\text{-}Pr_2$)[21] and ROMP monomers 5-norbornene-2-yl-$CH_2O(CH_2)_5P(oct)_2$ (**1**, NBP) and 2-[4′-(5-norbornenylmethoxycarbonyl)biphenyl-4-yl]-5-(4-*t*-butylphenyl)-1,3,4-oxadiazole (**2**, NBPBD) were synthesized according to literature procedures.[9,12] CdSe quantum dots were prepared and isolated as described.[9,10] Synthesis of ZnS-overcoated CdSe nanoclusters via incubation of size-selected CdSe clusters in the presence of dimethylzinc and bis(trimethylsilyl) sulfide was recently reported.[17]

Light-scattering gel-permeation chromatography (LS-GPC) analysis was carried out at room temperature employing a Rheodyne Model 7125 sample injector, a Kratos Spectroflow 400 pump, Shodex KF-802.5, 803, 804, 805, and 800P columns, a Knauer differential refractometer, and a Spectroflow 757 absorbance detector on samples 0.1−0.3% (w/v) in CH_2Cl_2. Viscometric GPC measurements were carried out on a Kratos Spectroflow 408 pump, using two Jordi-Gel DVB mixed-bed columns in series and a Viscotek differential refractometer/viscometer H-500 on samples 0.1−0.2% (w/v) in THF. All samples were filtered through a Millex-SR 0.5 μm filter in order to remove particulates. GPC columns were calibrated versus commercially available polystyrene standards (Polymer Laboratories Ltd.) ranging from 1206 to 1.03×10^6 g/mol MW. Light-scattering measurements were analyzed using ASTrette 1.2 (Wyatt Technology Corp.); viscometric measurements, using Unical 4.03 (Viscotek).

Solution fluorescence experiments were performed on a SPEX Fluorolog-2 spectrometer, using front-face collection with 0.4 mm slits. Fluorescence spectra were collected within a 100 nm window centered on the wavelength of the principal absorption band, with excitation 100 nm to the blue. For example, data for ∼45 Å clusters (absorbance λ_{max} 580 nm) were collected between 530 and 630 nm with 480 nm excitation. Fluorescence spectra of thin films were performed using the same parameters, with right-angle detection and 1 mm slits. Optical absorption spectra were obtained at room temperature on a Hewlett-Packard 8452A diode array spectrometer, using 1 cm quartz cuvettes. Transmission electron microscopy (TEM) was performed on a JEOL 200 CX in bright field at 100 kV.

General Procedure for Polymer Synthesis. The synthesis of the $[NBPBD]_{300}[NBP]_{20}$ diblock copolymer (see Table 1) is given as an example. (The numerical subscripts following the monomer name indicate the number of equivalents of a monomer that are added to 1 equiv of the alkylidene initiator. Previous studies with these initiators have shown that in many cases the number of equivalents added approximately equals the actual degree of polymerization of the individual blocks.)[22] A solution of $Mo(CHCMe_2Ph)(NAr)(O\text{-}t\text{-}Bu)_2$ **3** (0.40 mg, 0.73 μmol) in THF (1 mL) was added all at once to a rapidly stirred solution of NBPBD (110 mg, 0.218 mmol) in THF (7 mL). After 1 h, a solution of NBP (6.6 mg, 15 μmol) in THF (1 mL) was added, and the mixture was stirred for 1 h before it was quenched by addition of 3 drops of PhCHO. The solution was stirred for 1 h, then reduced in volume, and added dropwise to degassed MeOH (10 mL). The white solid was collected by filtration, washed with MeOH, and dried under high vacuum to yield 109 mg (93%).

Extent of Incorporation of CdSe Nanoclusters into Polymers. In a representative experiment, a solution of $[NBPBD]_{300}$ (5 mg) in THF (2.0 mL) was added to a solution of CdSe nanoclusters (0.76 mg) in THF (1 mL). The mixture was stirred for 1 h and the solvent was removed in vacuo. Extraction of the residue with 10 mL of hexane yielded a pale orange solution, which was diluted to 2.0 mL. The UV−visible spectrum of the extract was measured and the concentration of polymer-free nanoclusters in solution calculated by interpolation against a Beer's law plot.

Preparation of Samples for TEM Analysis. Samples were prepared from thin films (<100 nm) static-cast from solution unless otherwise noted. Solutions for static-cast samples were typically made up as follows. To $[NBPBD]_{300}$-$[NBP]_{20}$ copolymer (0.833 mg) in 1:1 THF−toluene (total volume 1.88 mL) was added 0.062 mg of CdSe nanoclusters to obtain a solution 7.4% (w/w) cluster to polymer, and 0.05% (w/w) polymer to solvent. The solution was allowed to equilibrate for 24 h. Films were then cast by dropping ∼100 μL of the solution onto cleaved mica coated with ∼10 nm of evaporated carbon. The rate of solvent evaporation from the latter was reduced by addition of 3 mL of THF to the casting chamber, which was covered and left to stand, typically for 8 h. The films were removed from the drybox and scored into 1 mm × 1 mm pieces, which were then floated onto deionized water and picked up with 200 mesh copper TEM grids. Film thicknesses were estimated to be in the range of 30−50 nm on the basis of their silver interference color floating on water. The TEM samples were imaged perpendicular to the film plane. Solutions for spin-cast samples were made up in the same way, but at higher concentrations, typically 1 wt % polymer to solvent. Films were cast at 1200 rpm onto 1 cm × 1 cm carbon-coated mica substrates.

Results

Monomer Synthesis and Properties. We recently described the design and synthesis of monomer **1**, a dioctylphosphine derivative of 5-norbornene-2-methanol.[9] This monomer (abbreviated as NBP) is obtained as a clear, colorless oil, which is purified by distillation under high vacuum and stored at −40 °C in the drybox. We have also recently developed a high-yield route to the oxadiazole-functionalized norbornene monomer **2** (abbreviated as NBPBD).[12] The structures of the two monomers and that of the pure hydrocarbon monomer methyltetracyclododecene (MTD) are illustrated below.

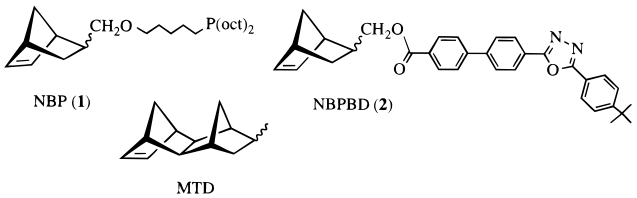

Polymer Synthesis. Syntheses of NBPBD homopolymer and MTD−NBP diblock copolymers have been described.[9,12] Homopolymers of NBPBD are written as $[NBPBD]_n$, where n represents the number of equivalents of monomer used per equivalent of initiator. Almost certainly they do not have regular structures, but probably a mixture of cis and trans double bonds and head-to-head, head-to-tail, and tail-to-tail arrangements of the repeat unit,[22,23] as well as endo/exo isomers of the monosubstituted norbornenes. The structures given for the polymers therefore are simplified representations. Polymerizations were carried out in THF, using $Mo(CHCMe_2Ph)(NAr)(O\text{-}t\text{-}Bu)_2$ (**3**) as the initiator (Scheme 1). Diblock copolymers were prepared by sequential addition of the oxadiazole- and phosphine-functionalized monomers, NBPBD and NBP, respectively, to the ROMP initiator. Polymerizations were terminated by addition of benzaldehyde, cleaving the polymer chain from the metal in a Wittig-like reaction. Polymers were precipitated by dropwise addition of the concentrated reaction mixture to degassed methanol and analyzed by GPC.

Polymerization Results. GPC analysis of NBPBD homopolymers typically indicated narrow, unimodal molecular weight distributions with a polydispersity index (PDI) of 1.03−1.05. $[NBPBD]_n[NBP]_m$ copolymers showed a bimodal molecular weight distribution with two narrow peaks, as previously observed for $[MTD]_{300}$-$[NBP]_{20}$ copolymers.[9] The origin of bimodality in the MTD−NBP system was unclear, though an extrinsic factor was suggested by the variability in the proportion of the two peaks. Contamination by oxygen, which can cause coupling of two polymer chains (eq 1),[24] was ruled out on the basis of the high ratios of molecular weights of the two peaks: GPC analysis by viscometry indicated molecular weight ratios of 2−10:1, rather than 2:1. In the case of the NBPBD−NBP copolymers, molecular weight ratios gauged by viscometry were likewise variable, but more accurate light-scattering measurements consistently indicated ratios of 2:1.

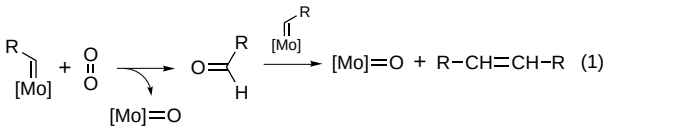

This evidence, and the observed decline in the amount of high-molecular weight material following freeze−thaw−degassing of the phosphine monomer, point toward contamination of **1** by a volatile contaminant, such as oxygen, that can effect bimolecular coupling of two polymer chains. The contaminant is extraordinarily tenacious, possibly owing to the viscosity of **1**; complete disappearance of the high-molecular weight peak was not effected by successive freeze−thaw−degassing steps but required prolonged exposure of rapidly stirred, neat **1** to dynamic vacuum. Copolymers of NBPBD and NBP (and MTD−NBP) prepared after such treatment exhibited narrow, unimodal GPC traces, with a PDI of ∼1.07.

Passivation of (CdSe)ZnS Clusters with Molecular Donors. The relative passivating abilities of a range of potential donors for (CdSe)ZnS nanoclusters were examined by fluorometry. Screening experiments were undertaken with ZnS-overcoated clusters in order to gauge their affinity for $P(oct)_3$ relative to "hard" phosphine oxide and amine donors, as well as molecular PBD (the oxadiazole nitrogens of which are potential ligands). These experiments are summarized in Figure 1. Successive addition of molecular PBD, NEt_3, and $O{=}P(oct)_3$ to cluster solutions causes successive decreases in emission. Fluorescence is completely restored, however, by subsequent addition of $P(oct)_3$. These results suggested that phosphine-functionalized polymers would provide suitable hosts for (CdSe)ZnS clusters.

Incorporation of CdSe and (CdSe)ZnS Nanoclusters into ROMP Polymers. The extent of cluster uptake was assessed by mixing the clusters and the polymers in THF and then removing the solvent. Extraction of the solid residue with hexane removes any polymer-free clusters, the amount of which was then quantified by reference to a Beer's law plot for the relevant cluster batch, as previously described.[9] Uptake of CdSe nanoclusters by $[NBPBD]_{300}$ is incomplete (amounting to 80% of the original loading level) but is

Scheme 1. Sequential Polymerization of Oxadiazole- and Phosphine-Functionalized Norbornene Derivatives

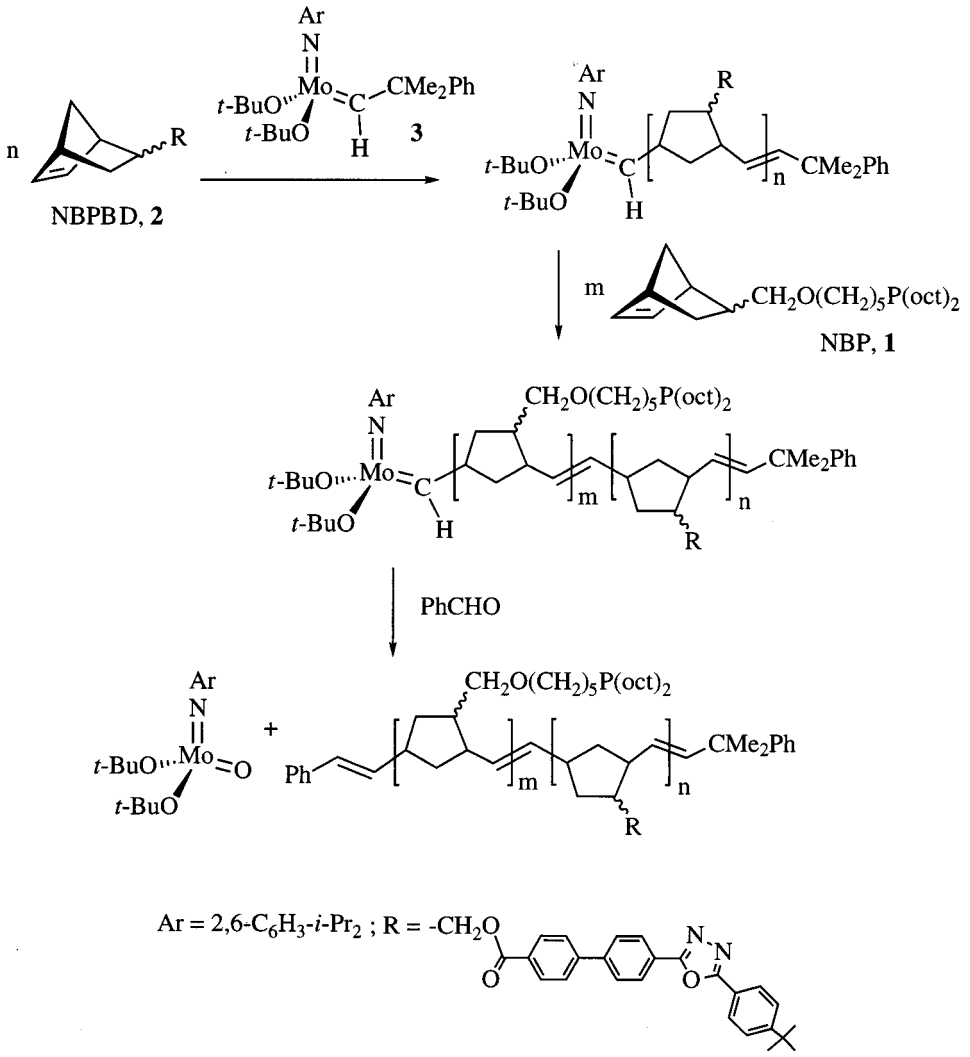

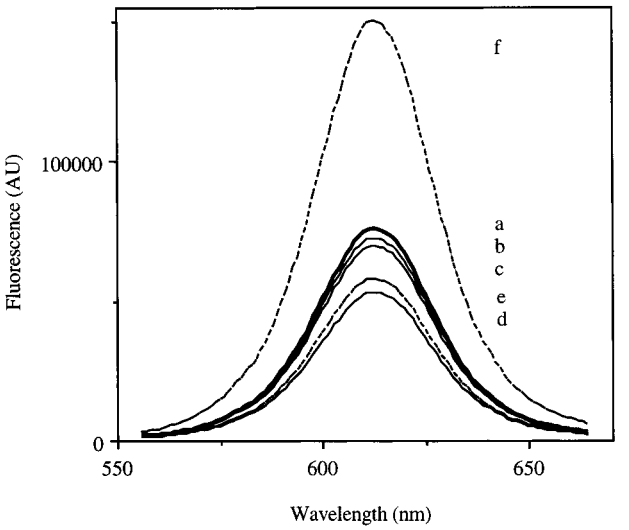

Figure 1. Comparative effects of added donors on (CdSe)-ZnS cluster fluorescence: emission spectra are shown (a) of free clusters in THF; (b) 2 h after addition pf oxadiazole, (c) 2 h after addition NEt_3 to solution from (b); (d) 2 h after addition $O{=}P(oct)_3$ to solution (c); (e) immediately after addition $P(oct)_3$ to solution (d); and (f) of solution (e) after 2 days.

quantitative for $[NBPBD]_{300}[NBP]_{20}$; uptake of (CdSe)-ZnS nanoclusters by either polymer is quantitative.

Changes in nanocluster size are signaled by shifts in the wavelength of the absorption maximum. The structural integrity of the clusters was thus readily monitored by visible absorption spectroscopy, while electronic passivation was monitored by fluorescence. No change in the absorption spectrum follows incorporation of either type of nanocluster into NBPBD homopolymer or NBPBD−NBP copolymers, indicating that the structural integrity of the clusters is unaffected. The effect of incorporation of both cluster types into NBPBD homopolymer and NBPBD−NBP copolymer is summarized in Figure 2. Photoluminescence slowly diminishes for CdSe clusters incorporated into $[NBPBD]_{300}$ but is enhanced in $[NBPBD]_{300}[NBP]_{20}$. (CdSe)-ZnS nanoclusters are comparatively insensitive to polymer type, and changes are much smaller, although the same trend is observed.

Transmission Electron Microscopy. TEM images reveal the morphological behavior of thin films of the NBPBD−NBP block copolymer containing either CdSe or (CdSe)ZnS nanoclusters. Films cast from THF showed gross variations in film thickness, whereas films from 1:1 THF−toluene mixtures were more uniform; all micrographs shown here were obtained using samples cast from the latter solvent mixture. When added to NBPBD homopolymer, both types of nanoclusters segregate into hexagonally packed domains of irregular shape and size, 10−200 nm in their largest in-plane dimension, which are randomly spaced over the polymer matrix (Figure 3). The nanoclusters themselves are

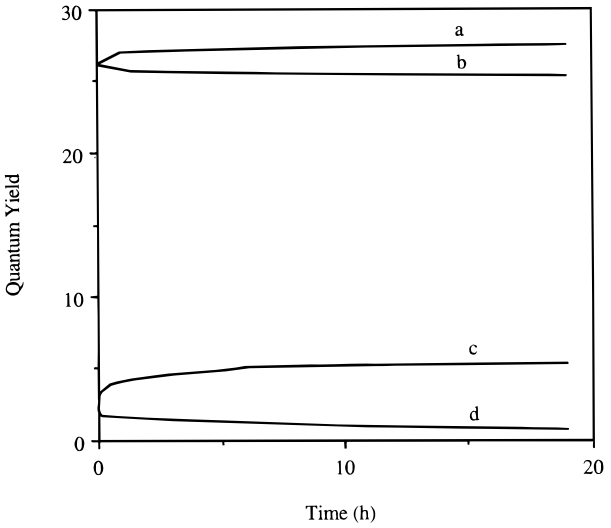

Figure 2. Time dependence of fluorescence following incorporation of dots into polymers: (a) emission of (CdSe)ZnS nanoclusters in $[NBPBD]_{300}[NBP]_{20}$; (b) (CdSe)ZnS nanoclusters in $[NBPBD]_{300}$; (c) CdSe nanoclusters in $[NBPBD]_{300}$-$[NBP]_{20}$; (d) CdSe nanoclusters in $[NBPBD]_{300}$.

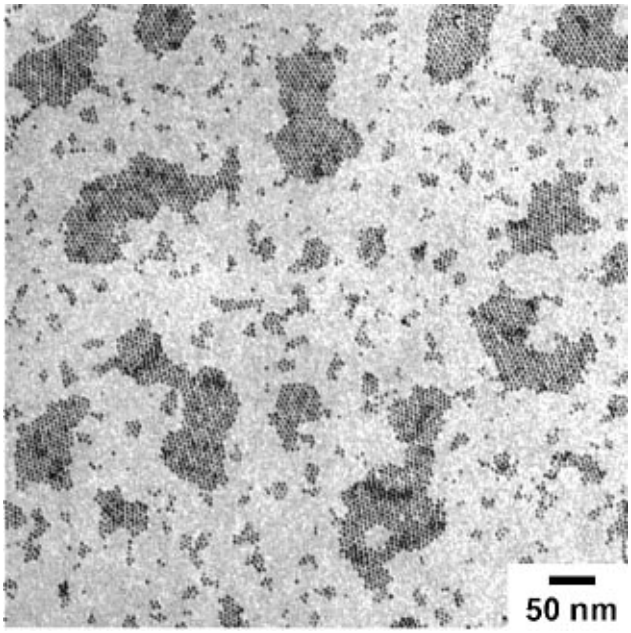

Figure 3. Transmission electron micrograph of CdSe nanoclusters forming domains of irregular size and shape in a $[NBPBD]_{300}$ homopolymer thin film.

markedly uniform in size and are separated from each other by the presence of the trioctylphosphine capping layer. Greater long-range order is observed in films of CdSe nanoclusters in $[NBPBD]_{300}[NBP]_{20}$ block copolymer, in which the nanoclusters assemble into domains of more uniform shape and dimensions: 15−20 nm wide and 25−100 nm long nanocluster-rich channels are periodically spaced 50−60 nm apart in a nanocluster-poor matrix (Figure 4). Films of $[NBPBD]_{300}[NBP]_{20}$ containing (CdSe)ZnS nanoclusters, however, exhibit a morphology similar to that of nanoclusters in the homopolymer, with isolated, 100−800 nm wide regions of nanoclusters randomly separated by equally large regions containing few or no nanoclusters, as shown in Figure 5. When block copolymer films containing (CdSe)ZnS nanoclusters were spin-cast, solvent evaporation took place in seconds and produced small aggregates of nanoclusters, 5−20 nm in diameter, uniformly dispersed

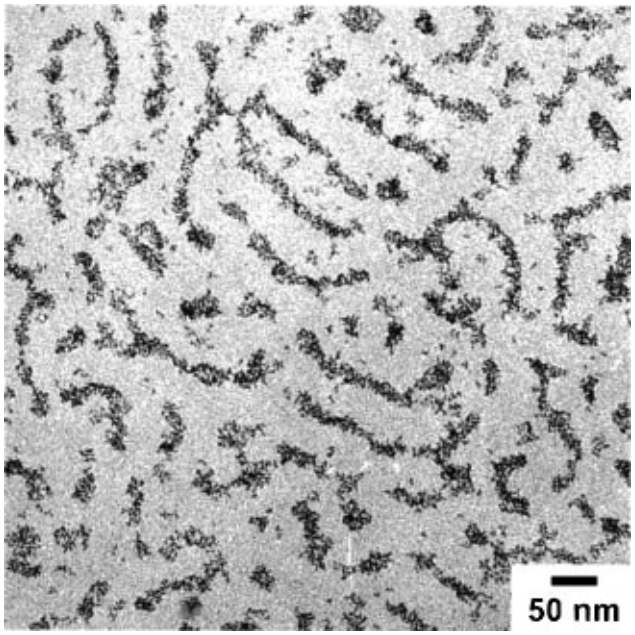

Figure 4. Electron micrograph of CdSe nanoclusters in a $[NBPBD]_{300}[NBP]_{20}$ copolymer thin film, showing development of a microdomain morphology.

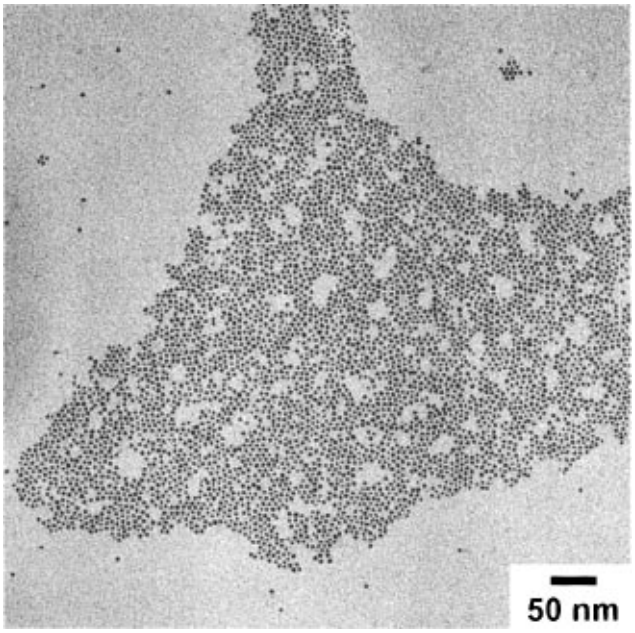

Figure 5. Electron micrograph of (CdSe)ZnS nanoclusters in a $[NBPBD]_{300}[NBP]_{20}$ copolymer thin film, showing larger and more irregular nanocluster domains than Figure 4.

but with no long-range order (Figure 6). There was also no indication of film thickness variations.

Discussion

Incorporation of CdSe nanoclusters in NBPBD homopolymer results in diminished fluorescence (Figure 2) and, over 8 h in solution, complete quenching of emission. A similar effect was observed in our original work following incorporation of nanoclusters into the pure hydrocarbon polymer $[MTD]_{300}$. Diminished passivation in each case is attributed to disruption of the dynamic equilibrium between free and bound cluster capping groups as a consequence of diffusion constraints introduced by the presence of the polymer in solution. Where the clusters are not tethered to the polymer, independent diffusion of cluster and capping groups

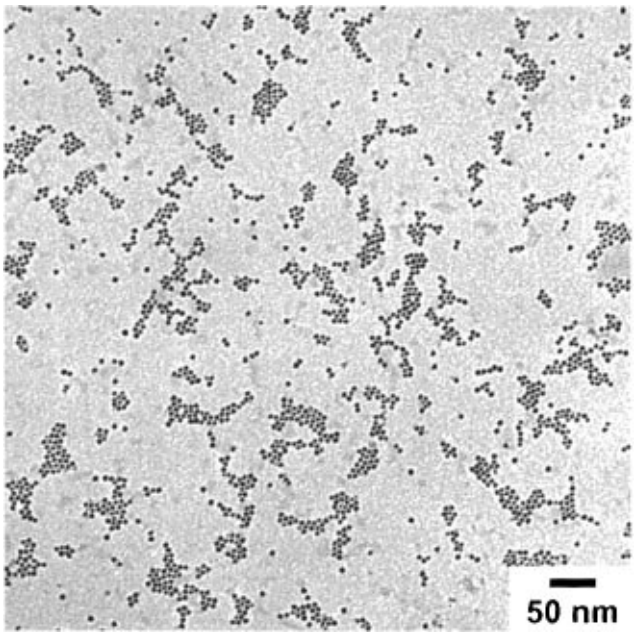

Figure 6. Electron micrograph of (CdSe)ZnS nanoclusters in a spin-cast $[NBPBD]_{300}[NBP]_{20}$ copolymer thin film. Rapid evaporation of solvent apparently suppresses formation of highly aggregated nanocluster domains.

through the polymer matrix can occur, shifting the equilibrium in favor of free ligand and depassivated nanoclusters. The similarity in behavior between NBPBD and MTD homopolymers indicates that the potentially ligating diazole groups on the former have negligible affinity for CdSe sites. This view is substantiated by TEM analysis of CdSe nanoclusters in $[NBPBD]_{300}$, which show macrophase separation of the nanoclusters (Figure 3), indicating that the self-affinity of the nanoclusters is stronger than their affinity for any group in the polymer matrix.

Incorporation of CdSe nanoclusters in NBPBD−NBP copolymers, as with the MTD−NBP polymers, enhances cluster emission. This increase reflects the improved electronic passivation effected by binding of polymer phosphine to vacant surface sites on incompletely passivated clusters present in the original sample. Sustained increases in emission are attributed to a process of self-assembly in solution, with progressively more surface sites on the clusters being taken up by polymer-bound phosphine. Binding of nanoclusters to NBP blocks is further implied by the morphological picture of well-defined and periodically spaced nanocluster regions (Figure 4), whose dimensions correlate with the sizes of the NBPBD and NBP blocks; this morphology presumably is imposed by microphase separation of NBPBD blocks from nanocluster-bearing NBP blocks.

ZnS-overcoated nanoclusters offer considerably "harder" Lewis basic surface sites for coordination of capping groups (whether of molecular or polymeric origin) than do the original CdSe nanoclusters. The ZnS shell, itself a capping layer, confers a very high degree of electronic passivation on the CdSe core and thus renders cluster emissivity less sensitive to the integrity of the organic capping layer than "bare" CdSe clusters. More critical are issues of steric insulation and (in the extreme) solubility. Loss of organic capping groups reduces interdot repulsion, and agglomeration or scavenging of smaller clusters by larger ones can occur if the ZnS surfaces come into contact. The lower affinity of $P(oct)_3$ and $O{=}P(oct)_3$ for the ZnS shell is manifest in the tendency of these clusters to precipitate if purified by the protocol established for CdSe nanoclusters. Thus, where the latter are precipitated three times from BuOH−hexanes to effect size selection and removal of excess phosphine/phosphine oxide, (CdSe)ZnS nanoclusters tolerate only one cycle of precipitation before their solubility in hexanes is lost. It should be noted that solubility in THF is less readily compromised, probably because the Lewis basicity of the furan oxygen permits the solvent itself to augment the capping layer.

Redesign of the polymer host to incorporate harder donors than phosphine was considered in view of the change from soft, diffuse Cd surface sites to harder Zn sites. A series of potential donor molecules was screened for binding affinity and passivating properties. Relative passivating and binding properties of potential donors are readily assayed by fluorometry, via addition of free ligand to cluster solutions containing alternative donors. Addition of $P(oct)_3$ to solutions containing CdSe clusters and free $O{=}P(oct)_3$, for example, causes a dramatic increase in emission, indicating both that the phosphine donor outcompetes the phosphine oxide for coordination to the clusters and that $P(oct)_3$ is a more effective passivating group than $O{=}P(oct)_3$.[9] (This is fully consistent with the relative affinities expected on the basis of hard−soft Lewis acid−base formalism, reflecting the high affinity of the diffuse Cd orbitals for soft donors such as phosphorus.) As indicated in Figure 1, molecular PBD is the weakest donor screened (problems of nanocluster sequestration into NBPBD domains were therefore not anticipated) and has little effect of fluorescence. Amine donors are well-established in the coordination chemistry of zinc and were successfully employed as passivating groups in early work on CdS clusters.[25] Triethylamine proves a more effective ligand than PBD, though less so than either $O{=}P(oct)_3$ or $P(oct)_3$; however, it causes a slight decrease in fluorescence. Similarly, $O{=}P(oct)_3$ quenches emission of (CdSe)ZnS clusters to some extent, as indeed found for CdSe nanoclusters.[9] On addition of $P(oct)_3$ to cluster solutions containing these ligands, the onset of recovery is immediate, and significant increases in emission occur over time in solution. This key observation indicates that $P(oct)_3$ is an effective donor for (CdSe)ZnS clusters, outcompeting harder amine and phosphine oxide donors for coordination to surface sites. This alkylphosphine may in fact be a relatively "hard" donor; the conventional view of P as a soft donor ligands derives in part from the ubiquity of less basic arylphosphines in the literature. The hardness of the Zn surface sites may also be mitigated by interaction with the surrounding soft S donors. The passivating properties of $P(oct)_3$ are in any case unmatched by any other donors screened, and NBPBD−NBP copolymers were therefore investigated as hosts for these hybrid quantum dots.

Incorporation of (CdSe)ZnS nanoclusters in NBPBD homopolymer causes a slight decline in solution fluorescence, as expected, though the decrease is less pronounced than that found for the less well-shielded CdSe nanoclusters. TEM images of thin films show macrophase separation similar to that found for CdSe nanoclusters (Figure 3), with large and irregular domains of nanoclusters distributed throughout the polymer matrix. The solution fluorescence of (CdSe)ZnS nanoclusters is enhanced in NBPBD−NBP copolymers, leading us to expect segregation of nanoclusters in phosphine-rich domains by analogy to the CdSe systems; however, we consistently see the macrophase-

separated morphology as in Figure 5. This implies that the self-affinity of the clusters is greater than their affinity for the phosphine domains within the polymer matrix: the affinity of the nanoclusters for polymer phosphine is clearly insufficient to overcome the self-preference of the clusters under conditions of slow casting. Macrophase separation of aggregated nanoclusters is not observed in spin-cast films, however, in which evaporation is complete in seconds (Figure 6). Formation of extended aggregates of dots during slow evaporation may be due to collapse of the capping layer following loss of volatile THF donors, which in solution swell the capping layer and enhance steric insulation of the nanoclusters.

Sequestration of highly monodisperse, electronically passivated semiconductor nanoclusters within electronically passivating microdomains in a charge-transporting matrix represents a significant advance in the fabrication of nanostructured polymer−cluster composites. These materials display considerable promise as combined electron-transport and emitter layers in light-emitting devices, in which morphological control permits unravelling of the relationship between device performance and composite morphology. We have now begun to turn our attention to the potential utility of related composites for photovoltaic applications.

Acknowledgment. This work was supported by the National Science Foundation (Grant DMR 87 19217) and in part by the MRSEC Program of the National Science Foundation under award DMR 94-00334.

References and Notes

(1) Adachi, C.; Tsutsui, T.; Saito, S. *Appl. Phys. Lett.* **1989**, *55*, 1489.
(2) Kido, J.; Kohda, M.; Okuyama, K.; Nagai, K. *Appl. Phys. Lett.* **1992**, *61*, 761.
(3) Burn, P. L.; Kraft, A.; Baigent, D. R.; Bradely, D. D. C.; Brown, A. R.; Field, R. H.; Gymer, R. W.; Holmes, A. B.; Jackson, R. W. *J. Am. Chem. Soc.* **1993**, *115*, 10117.
(4) Colvin, V. L.; Schlamp, M. C.; Alivisatos, A. P. *Nature* **1994**, *370*, 354.
(5) Dabbousi, B. O.; Bawendi, M. G.; Onitsuka, O.; Rubner, M. F. *Appl. Phys. Lett.* **1995**, *66*, 1316.
(6) Lin, C. P.; Tsutsui, T.; Saito, S. *New Polym. Mater.* **1995**, *4*, 277.
(7) Pommerehne, J.; Vestweber, H.; Guss, W.; Mahrt, R. F.; Bassler, H.; Porsch, M.; Daub, J. *Adv. Mater.* **1995**, *7*, 551.
(8) Brus, L. *Appl. Phys. A* **1991**, *53*, 465.
(9) Fogg, D. E.; Radzilowski, L. H.; Blanski, R.; Schrock, R. R.; Thomas, E. L. *Macromolecules* **1997**, *30*, 417.
(10) Murray, C. B.; Norris, D. J.; Bawendi, M. G. *J. Am. Chem. Soc.* **1993**, *115*, 8706.
(11) Kido, J.; Hongawa, K.; Okuyama, K.; Nagai, K. *Appl. Phys. Lett.* **1993**, *63*, 2627.
(12) Boyd, T. J.; Geerts, Y.; Lee, J.-K.; Fogg, D. E.; Lavoie, G. G.; Schrock, R. R.; Rubner, M. F. *Macromolecules* **1997**, *30*, 3553.
(13) Brown, A. R.; Bradley, D. D. C.; Burroughes, J. H.; Friend, R. H.; Greenham, N. C.; Burn, P. L.; Holmes, A. B.; Kraft, A. *Appl. Phys. Lett.* **1992**, *61*, 2793.
(14) Kim, D. U.; Tsutsui, T.; Saito, S. *Polymer* **1995**, *36*, 2481.
(15) Strukelj, M.; Miller, T. M.; Papadimitrakopoulos, F.; Son, S. *J. Am. Chem. Soc.* **1995**, *117*, 11976.
(16) Pei, Q.; Yang, Y. *Chem. Mater.* **1995**, *7*, 1565.
(17) Dabbousi, B. O.; Rodriguez-Viejo, J.; Mikulec, F. V.; Heine, J. R.; Mattoussi, H.; Jensen, K. F.; Bawendi, M. G. *J. Phys. Chem., B* **1997**, *101*, 9463.
(18) Hines, M. A.; Guyot-Sionnest, P. *J. Phys. Chem.* **1996**, *100*, 468.
(19) Kortan, A. R.; Hull, R.; Opila, R. L.; Bawendi, M. G.; Steigerwald, M. L.; Carroll, P. J.; Brus, L. E. *J. Am. Chem. Soc.* **1990**, *112*, 1327.
(20) Dabbousi, B. O.; Radzilowski, L. H.; Fogg, D. E.; Mattousi, H.; Schrock, R. R.; Rubner, M. F.; Thomas, E. L.; Bawendi, M. G. *J. Appl. Phys.*, in preparation.
(21) Schrock, R. R.; Murdzek, J. S.; Bazan, G. C.; Robbins, J.; DiMare, M.; O'Regan, M. *J. Am. Chem. Soc.* **1990**, *112*, 3875.
(22) Schrock, R. R. *Acc. Chem. Res.* **1990**, *24*, 158.
(23) Schrock, R. R. In *Ring-Opening Polymerization*; Brunelle, D. J., Ed.; Hanser: Munich, 1993.
(24) Feast, W. J.; Gibson, V. C.; Khosravi, E.; Marshall, E. L.; Mitchell, J. P. *Polymer* **1992**, *33*, 872.
(25) Dannhauser, T.; O'Neil, M.; Johansson, K.; Whitten, D.; McLendon, G. *J. Phys. Chem.* **1986**, *90*, 6074.

MA970626I